Comparison of morphological and optical properties of nanocrystalline tin selenide powder and thin films

DEEP SHIKHA[a,b], R. P. CHAUHAN[c], JEEWAN SHARMA[d,*]
[a]*Department of Physics, Maharishi Markandeshwar University, Mullana, Ambala-133207 India*
[b]*Ambala College of Engineering and Applied Research, Mithapur-133101 India*
[c]*Department of Physics, National Institute of Technology, Kurukshetra-136119 India*
[d]*Department of Nanotechnology, Shri Guru Granth Sahib World University, Fatehgarh Sahib-140406 India*

Chemical bath deposition technique has been used to synthesize tin selenide (SnSe) powder and thin films. The synthesized SnSe has been found to have grain size less than 100 nm. The SnSe thin films are deposited on glass substrates in an aqueous alkaline medium using sodium selenosulphate as Se^{2-} ion source. To assess the quality of the SnSe thin films the morphology of SnSe has been studied by using scanning electron microscopy (SEM) at different resolutions and crystallite size has been calculated by X-ray diffraction (XRD). Information of the strain and the particle size has been obtained from the full widths at half maximum (FWHM) of the diffraction peaks. The band gap of nanocrystalline SnSe has been calculated using absorbance curves and blue shift in the fundamental edge has been observed.

(Received March 19, 2012; accepted July 19, 2012)

Keywords: Morphological, Chemical bath deposition, Tin selenide thin films

1. Introduction

SnSe has been studied in the form of both single crystal [1] and thin films [1-3]. Tin selenide (SnSe) has been used as memory switching devices, holographic recording systems and infrared electronic devices [4-6]. It could also be used in photo-electrochemical cells, decreasing the photo corrosion reaction [5]. Tin selenide exists as a layered compound with an orthorhombic crystal structure. Different methods of preparation have been described in the literature: chemical bath deposition [2], vacuum evaporation, chemical vapor deposition, electrodeposition [4,1-3] and solvothermal routes [1]. Chemical bath deposition is the cheapest known technique for preparation of powder and thin films. It is a slow process, which facilitates a better orientation of the crystallites with an improved grain structure. Depending on the deposition condition, the film growth can take place by ion–ion condensation or by adsorption of colloidal particles (cluster by cluster) from the solution onto substrates. Many of these films proved to be of comparable quality with those produced by other sophisticated and expensive methods. Present paper reports the preparation and morphological study of the tin selenide both in powder and thin film form obtained by a simple chemical route.

2. Experimental details

Tin selenide thin films were deposited onto cleaned, spectroscopic grade glass substrates. All chemicals used were of AR grade. To synthesize nanocrystalline SnSe we have employed the chemical bath deposition (CBD) technique using tin chloride and sodium selenosulphate as precursors of Sn^{2+} and Se^{2-} ions in the reaction system. To prepare sodium selenosulphate solution, 15 g of sodium sulfite in 200 ml water was refluxed with 5 g of selenium for almost 10 hours at 75^0C. The mixture remained under constant stirring throughout the reflux process. Selenosulphate is produced according to the following reaction:

$$Na_2SO_3 + Se \rightarrow Na_2SeSO_3 \quad (1)$$

Unreacted selenium is filtered off and selenosulphate solution is placed in air tight bottle. It is recommended to make small volumes of selenosulphate stock solution to be used within 3–4 days. To deposit SnSe, sodium hydroxide (1M) solution in deionized water is prepared. This solution is used to maintain alkaline media of pH at about 11.2. In a beaker sodium hydroxide is added drop wise to 0.94 g of tin chloride dissolved in 10 ml water to obtain an alkaline media of pH 11.2. Then 10 ml of sodium selenosulphate solution is introduced into the beaker and glass substrates are mounted vertically in the bath. The film growth was carried out at 42° C. A dark brown precipitate gradually fills the bath and turns black after 20 min. During deposition period the beaker was kept undisturbed for a time period of 1.5 hours. To prepare SnSe in powder form, the solid phase after removing the film will be isolated by filtration and finally dried in hot bath, from the residue solution. This solid phase (powder) consist of SnSe nanocrystals. Surface morphological and compositional analyses were carried out using a scanning electron microscope. The XRD patterns were collected with Rigaku

Geigerflex equipment using nickel filtered CuKα radiation (λ=1.54 Å). The absorption spectra were recorded using double beam spectrophotometer [SPECORD-250] in the transmission range 200-800 nm for both samples.

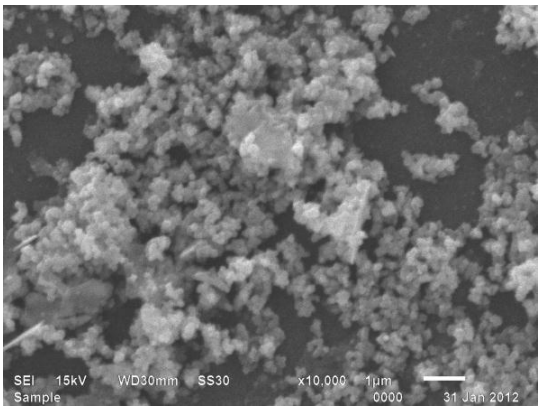

Fig. 1. SEM micrographs of SnSe powder.

2.1 Chemical aspects of deposition process

In chemical bath deposition the chemical deposition of tin selenide films was based on two important properties of selenosulphate. One is its complexing ability, much like the well known complexing ability of thiosulphate [7]. Tin selenosulphate complexes are formed in excess of selenosulphate. The other is the ability of selenosulphate to gradually release selenide ions upon hydrolytic decomposition, in alkaline media, as

$$SeSO_3^{2-} + OH^- \rightarrow HSe^- + SO_4^{2-} \quad (2)$$

$$HSe^- + OH^- \rightarrow Se^{2-} + H_2O \quad (3)$$

Then, the released selenide ions combine with the tin ions released from the tin selenosulphate complexes, upon hydrolysis, precipitating SnSe:

$$Sn^{2+} + Se^{2-} \rightarrow SnSe \quad (4)$$

The advantage in this case over other chemical baths is the combined role of selenosulphate ions both as a complexing agents for Sn^{2+} ions as well as a provider of selenide ions, instead of using one chemical as a complexing agent (EDTA, triethanolamine etc.) and a second chemical as a generator of selenide ions (H_2Se, selenourea etc.) [7]. Therefore, the fabrication of SnSe films is not only made more economic, but also chemically free of additional contaminants.

3. Results & discussion

SEM studies were carried out to assess the quality of the SnSe powder and thin films deposited on glass substrate. Figs. 1 and 2 show scanning electron micrographs of the synthesized SnSe powder and thin films. The SEM micrograph of powder contains particles with almost spherical shape aggregated severely. These results are in good agreement with others [8]. The SEM micrograph of film shows a distribution of particles which covers the surface of the substrate completely. No pin holes or cracks could be observed for that sample.

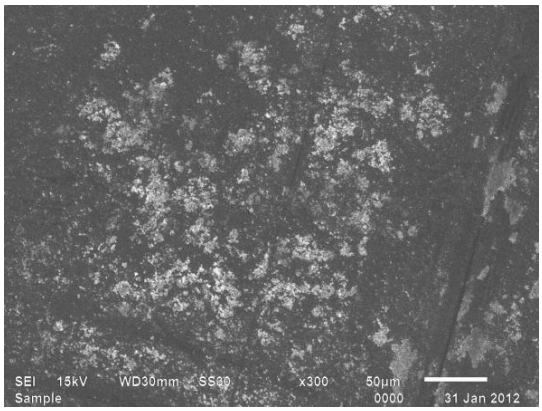

Fig. 2. SEM micrographs of SnSe thin film.

One can see the uniform distribution of grain size over total coverage of the substrate with a compact and fine grained morphology. This type of morphology has also been observed by others for nanocrystalline SnSe [2,3,9,10]. Clearly the crystalline size both in powder and thin film is of nanometer range. These results also confirm the results obtain from XRD data.

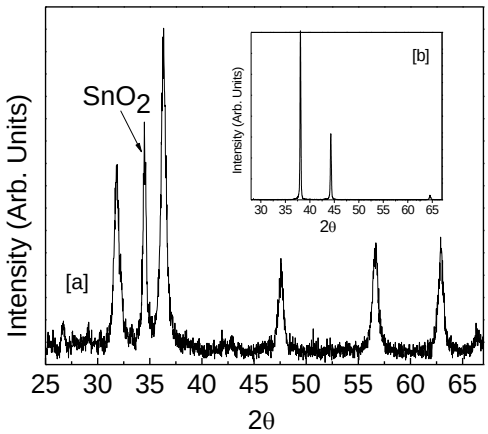

Fig. 3. XRD pattern of for SnSe [a] powder and [b] thin film.

Fig. 3 represents the diffraction pattern of SnSe for powder as well as thin film. The diffraction peaks of SnSe were observed at 2θ=38.06°, 44.28° and 64.6° for thin film and at 2θ=31.86°, 36.32°, 47.62°, 56.68° and 62.9° for powder. In powder SnSe an additional peak of SnO_2 is also observed [11] at 2θ=34.48°. The calculated *d*-values for

SnSe thin film are 2.363 Å, 2.043 Å and 1.442 Å and for powder these values are 2.812 Å, 2.4725 Å, 1.9113 Å, 1.625 Å and 1.478 Å. The observed *d*-values of both thin film and powder form are in good agreement with the standard values for the orthorhombic structure of SnSe [4,11]. Comparing the *d*-values with standard values indicates that {410} is the preferred orientation in these samples. The diffusion background and broad peak appearing at low angles are due to the amorphous glass substrate.

Information about strain and particle size are obtained from the full width at half maximum (FWHM) of the diffraction peaks. The FWHM (β) can be expressed as a linear combination of the contributions from the strain (ε) and particle size (L) as in relation:

$$\frac{\beta cos\theta}{\lambda} + \frac{1}{L} = \frac{\epsilon \sin\theta}{\lambda} \quad (5)$$

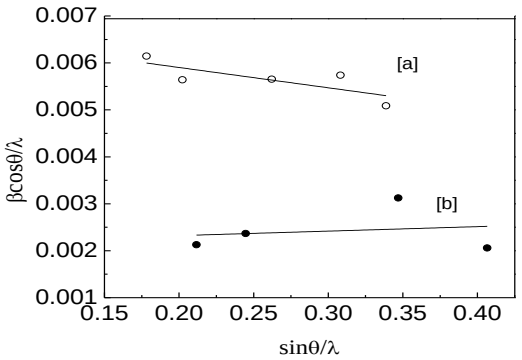

Fig. 4. Plot of (βcosθ)/λ vs. (sinθ)/λ for SnSe [a] powder and [b] thin film.

Fig. 4 represents the plots of (βcosθ)/λ vs. (sin θ)/λ for SnSe thin film and powder, which are straight lines. The amount of residual strain has been calculated using equation (5). Stress and strain are almost always present in thin films deposited on substrates. In the majority of cases, these stresses are residual stresses introduced into the system during deposition or subsequent processing. The negative value of residual strain indicates the compressive strain and the positive value indicates the tensile strain. In our case, there is tensile strain in thin film and compressive strain in powder form.

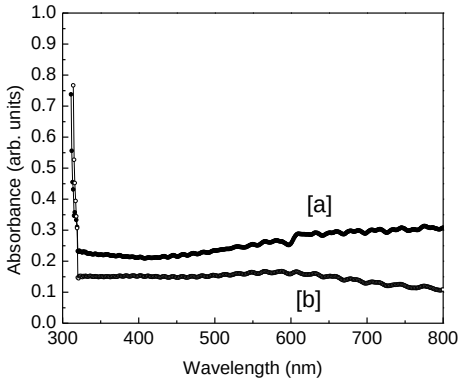

Fig. 5. Absorption spectra of SnSe [a] powder and [b] thin film.

The reciprocal of intercept on the (βcosθ)/λ axis gives the average particle size. In our case the particle size and strain calculated from Fig. 4 are listed in Table 1. The strain in thin film is much less than the powder this is possibly due to large crystalline size of grains in case of film.

Fig. 5 represents the absorption spectra of SnSe powder and thin film. The abrupt increase in absorption is due to glass substrate. These type of curves are also obtained by Okereke et al. for nanocrystalline SnSe [12]. From the absorption data, nearly at the fundamental absorption edge, the values of absorption coefficient (α), are calculated in the region of strong absorption using the relation:

$$\alpha = \frac{1}{d}\ln\left(\frac{1}{T}\right) \quad (6)$$

The fundamental absorption, which corresponds to the transition from valence band to conduction band, can be used to determine the band gap of the material. The relation between α and the incident photon energy ($h\nu$) can be written as [13]:

$$\alpha = \frac{A\left(h\nu - E_g\right)^n}{h\nu} \quad (7)$$

where A is a constant, E_g is the band gap of the material and the exponent n depends on the type of transition. The n may have values 1/2, 2, 3/2 and 3 corresponding to the allowed direct, allowed indirect, forbidden direct and forbidden indirect transitions, respectively. The exact value of band gap is calculated by extrapolating the straight line portion of the $(\alpha h\nu)^{1/n}$ vs $h\nu$ graph to the $h\nu$ axis.

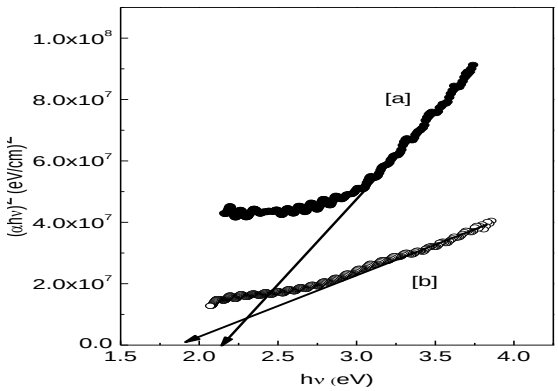

Fig. 6. Plot of $(\alpha h\nu)^2$ vs. energy for SnSe [a] powder and [b] thin film.

Fig. 6 shows the plots of $(\alpha h\nu)^2$ vs $h\nu$ for SnSe powder and thin films. The correct values of the band gap calculated from above figure are found to be (2.14 ± 0.01) eV and (1.89 ± 0.01) eV for powder and film respectively. The observed values of E_g are higher than the value of bulk band gap of SnSe [(1.2 ± 0.01) eV] [14] due to quantum confinement effects. N. Kumar *et al*. reported the band gap of SnSe thin films, deposited by thermal

evaporation technique, equal to 1.92 eV which is in good agreement with observed values [10]. Also the optical band gap of SnSe powder is greater than the thin film. This increase in band gap is supported by the fact that the crystallite size is less leading to greater extent of quantum confinement in powder. The narrow optical band gap in SnSe thin films as compared to SnSe powder indicates that it is more useful in photovoltaic applications.

Table 1. Structural and optical parameters of SnSe powder and thin film.

SnSe	Size (nm)	Strain (lin^{-2} m^{-4})	Band Gap (eV)
Powder	14.92	-4.32×10^{-3}	2.14 ± 0.01
Thin film	46.94	9.55×10^{-4}	1.89 ± 0.01

4. Conclusions

Preparation of nanocrystalline SnSe in thin film and in powdered form has been reported. SEM micrographs show the uniform distribution of grain size over total coverage of the substrate with a compact and fine grained morphology. Comparison of observed *d*-values with the standard values confirms orthorhombic structure of SnSe with {410} as preferred orientation in these samples. The average crystallite size for these samples has been calculated as 14.92 nm (powder) and 46.94 nm (thin film). Both the samples are found to be strained which may be due to the surface tension effect. Due to large crystallite size the thin film is less strained than powder. A direct optical band gap of 1.89 eV and 2.14 eV is found for SnSe thin films and powder respectively. The narrow optical band gap of thin film as compared to powder indicates its use in photovoltaic applications. From the above discussion, it is clear that the samples are nanocrystalline in nature and blue shift in the fundamental edge has been observed, due to the confinement effects arising from reduction in crystalline size.

Acknowledgements

The author acknowledges the support provided by Mr. S.C. Sood of Ambala College of Engineering, Mithapur for the completion of this work.

References

[1] W. Wang, Y. Geng, Y. Qian, C. Wang, X. Liu, Mater. Res. Bull., **34**, 403 (1999).
[2] Z. Zainal, N. Saravanan, K. Anuar, M. Z. Hussein, W. M. M. Yunus, Mater. Sci. Eng. B, **107**, 181 (2004).
[3] B. Subramanian, T. Mahalingam, C. Sanjeeviraja, M. Jayachandran, M. J. Chockalingam, Thin Solid Films, **357**, 119 (1999).
[4] Z. Zainal, S. Nagalingam, A. Kassim, M. Z. Hussein, W. M. M. Yunus, Solar Energy Mater. Solar Cells, **81**, 261 (2004).
[5] K. Zweibel, Solar Energy Mater. Solar Cells, **63**, 375 (2000).
[6] T. Lindgren, M. Larsson, S. Lindquist, Solar Energy Mater. Solar Cells, **33**, 377 (2002).
[7] I. Grozdanov, M. Najdoski, S. K. Dey, Mater. Lett., **38**, 28 (1999).
[8] Dong-Hau Kuo, Wei-Di Haung, Ying-Sheng Huang, Jiun-De Wu, Yan-Jih Lin, Thin Solid Films, **518 (24),** 7218 (2010).
[9] B. Subramanian, C. Sanjeeviraja, M. Jayachandran, Journal of Crystal Growth, **234**, 421 (2002).
[10] N. Kumar, V. Sharma, U. Parihar, R. Sachdeva, N, Padha, C. J. Panchal, J. Nano- Electron. Phys. **3 No.1,** 117 (2011).
[11] A. C. Bernardes-Silva, A. F. Mesquita, E. de Moura Neto, A. O. Porto, G. M. de Lima, J. D. Ardisson, F. S. Lameiras, Solid State Communications, **135**, 677 (2005).
[12] N. A. Okereke, A. J. Ekpunobi, Journal of Optoelectronics and Biomedical Materials, **3(3)**, 69 (2011).
[13] J. I. Pankove, Optical Processes in Semiconductors, Englewood Cliffs. NJ: Prentice-Hall (1971).
[14] J. P. Singh, Journal of materials science: materials in electronics, **2**, 105 (1991).

*Corresponding author: jeewansharma29@gmail.com